AN EVALUATION OF EQUIPMENT TO MEASURE DIRECTLY THE SKIN FRICTION FORCES ON A FLAT PLATE

A Thesis

Submitted to the Graduate Faculty

of the University of Minnesota

by

J. M. Wolff, Lieutenant U S N

In Partial Fulfillment of the Requirements

for the Degree of

Master of Science in Aeronautical Engineering

May 1956

ACKNOWLEDGMENTS

The author wishes to express his appreciation to Professor John D. Akerman for his advice and interest in this project; to the Aeronautical Engineering Department of the University of Minnesota for the extensive use of their subsonic wind tunnel; and to the members of the faculty and staff of the University for their aid and cooperation in solving the many problems that arise in an investigation of this type.

TABLE OF CONTENTS

LIST OF FREQUENTLY USED SYMBOLS

A - end area of floating element - ft^2

C_F - total skin friction coefficient

D - drag - lbs.

L - length of the test panel - ft.

p - pressure - lb/ft^2

P_B - barometric pressure - in. of Hg.

q - dynamic pressure - lb/in^2

R_N - Reynolds number

S - test panel area - ft^2

T - temperature - ^oR

t_D - dry bulb temperature - ^oF

t_w - wet bulb temperature - ^oF

u - velocity in the boundary layer - ft/sec.

U - free stream velocity - ft/sec.

x - distance from virtual origin to the leading edge of the test panel - ft.

y - vertical distance from the plate surface

δ - boundary layer thickness - ft.

μ - coefficient of viscosity - $\frac{lb.-sec.}{ft^2}$

ρ - density - $slugs/ft^3$

τ - shear stress - lbs/in^2

AN EVALUATION OF EQUIPMENT TO MEASURE DIRECTLY THE SKIN FRICTION FORCES ON A FLAT PLATE

ABSTRACT

An evaluation was made of an apparatus designed to measure directly the skin friction forces on a flat plate. A large portion of the surface of the plate was movable so that the skin friction forces would displace it against a restoring force. The displacement was calibrated as a force, and the drag of the surface read directly. The equipment was designed so that the surface of the movable section could be changed and the drag of plates of varying roughness measured.

In order to ascertain the effectiveness of this apparatus, the following aspects were investigated:

(1) To determine if the direct force measuring system actually measured the skin friction drag on the movable portion of the plate, results were compared to the drag obtained by a boundary layer survey. The agreement was found to be within eight per cent.

(2) The results obtained from the force measuring equipment were compared to empirical turbulent boundary layer drag equations. The agreement was found to be within two per cent.

(3) The sensitivity of the equipment was investigated by determining if small increases in surface roughness could be measured. The appartus showed an ability to measure the drag difference between a painted and unpainted glass surface.

(4) The repeatability of the drag measurements was excellent if no adjustment of the appartus was required between tests. It was found that large errors could be introduced if extreme care was not used in mounting and aligning the movable portion of the plate.

It was concluded that with reasonable care and experience with the apparatus, satisfactory results can be obtained.

AN EVALUATION OF EQUIPMENT TO MEASURE DIRECTLY THE SKIN FRICTION FORCES ON A FLAT PLATE

Introduction

Early experiments by Prandtl showed that for a body moving in a viscous fluid, particles next to the surface were pulled along at approximately the velocity of the surface. Particles farther away were also found to be pulled along, but with a velocity slightly less than that of the surface. The farther removed the particles were from the surface, the less effected they were by it. At a certain distance from the surface, the particles were no longer effected by the dragging forces of the surface; this distance was termed the boundary layer thickness. Prandtl found that this thickness was proportional to the square root of the fluid's kinematic viscosity. From this he surmised that for flow of a viscous fluid with small kinematic viscosity, the whole domain could be decomposed into two regions: (1) A thin layer next to the solid boundary where the velocity gradient is so large that the shear stress ($\tau = \mu \frac{du}{dy}$) is of the same order of magnitude as the pressure forces, and (2) outside of this thin layer where the velocity gradient is so small the fluid can be treated as non-viscous without any appreciable loss in accuracy.

The flow inside the boundary layer is of two types--laminar flow where the layers of fluid move essentially parallel to one another, and turbulent flow which is quite disordered. The velocity profiles, and hence the shear stresses, will be different for the two flows. The dragging effect of one layer of fluid on another is caused by the momentum change of a particle moving to a layer of different average momentum. For laminar flow the exchange of particles is accomplished by the random motion of the molecules. In turbulent flow the momentum transfer by molecular motion is augmented by the disordered motion of this type flow. This larger momentum transfer results in a greater velocity gradient at the solid boundary and, hence, larger shearing stresses.

The low skin friction drag associated with laminar flow is difficult to obtain on aircraft. This type of flow is unstable, and the point of transition to turbulent flow is effected by Reynolds number, pressure gradient, free stream turbulence, roughness, curvature, and temperature. Even carefully prepared surfaced such as an aircraft wing will collect sufficient dust and insects during taxi and take-off to produce early transition, leaving the major portion of the surface in turbulent flow (Ref. 1). It would appear then that the skin friction drag on all aircraft under service conditions would be almost entirely the higher drag associated with turbulent flow.

The theoretical calculation of the skin-friction drag is difficult. Several exact solutions to the Navier-Stokes equations for laminar flow on smooth surfaces do exist. The lack of information on the transition region from turbulent flow to the laminar sub-layer next to the surface and the friction laws in the sub-layer have thus far made any exact turbulent solutions impossible. One of the simplest cases of both laminar and turbulent boundary layers occurs on a flat plate at zero incidence. Under these conditions the pressure gradient down the plate is zero, and the free stream velocity will remain constant over the length of the plate. From the exact solution possible for laminar flow it can be seen that the skin friction drag is not appreciably effected by small pressure gradients. Thus, the skin friction drag on a flat plate will not differ greatly from that on a streamlined body, and results obtained for a flat plate will provide a basis for computing the drag on any body shape.

As mentioned above, the skin friction on a smooth flat plate with laminar flow can be obtained from a solution of the equations of motion. Several empirical formulas have been devised which agree closely with experimental results for turbulent flows (Ref. 2). These formulas apply to smooth plates, however, and surface roughness has a pronounced effect on skin friction drag. Extensive experimental results of the effect of roughness in pipes by Nikuradse[3] and extended to flat plates by Prantl and Schlichting[4] provide a means

of calculating the drag of a rough flat plate. These data are expressed as a function of the sand roughness used in the original pipe experiments which make it necessary to obtain an average equivalent sand roughness for the surface of interest. The equivalent sand roughness is a function of grain size, grain shape, and how closely the grains are packed. This value is difficult to determine for the type surfaces used on aircraft, and the problem of obtaining the skin friction drag on a slightly roughened plate remains.

Several methods of experimentally determining the drag of a flat plate are available and fall roughly into two categories: (1) Measurement of the effect of the plate on the airstream, and (2) direct force measurement of the drag of the airstream on the plate (Ref. 5). The effect of the plate on the airstream is generally measured by determining the velocity profile in the boundary layer with a pitot tube or hot wire anemometer. From the velocity defect the momentum loss suffered by the airstream can be calculated and represents the drag of the plate. Although this method produced satisfactory results, considerable time is required to obtain and reduce data for a large plate. The principle of measuring the effect of the airstream on the plate is quite simple. A portion of the surface is made movable so that the skin friction forces will displace it against some restoring force. The displacement can be calibrated to indicate force, and drag can then be read directly.

It is the purpose of this investigation to evaluate a direct force measurement device of this type. The apparatus was designed and built by Hendley[6] to measure the skin friction forces on test panels of different roughnesses. These test panels are easily interchanged which makes it possible to test a variety of surfaces without any modification of the equipment. The quantity of data required is small and little time is required for its reduction. This would appear to be a satisfactory method for determining the skin friction drag of rough plates without any knowledge of the degree of roughness of the surface. In order to ascertain the effectiveness of this apparatus, the following aspects were investigated:

Agreement with drag obtained from momentum loss--To determine if the direct force measuring system actually measured the drag on the test panels, results were compared to the drag obtained by the momentum loss method (Ref. 7).

Agreement with theory--To determine if the direct force measuring apparatus satisfied the requirements of a flat plate at zero incidence with no pressure gradient, results were compared to empirical turbulent skin friction equations.

Sensitivity--To determine the sensitivity of the system, the drag on a set of test panels was measured. A small increase in surface roughness was made and the drag measured again to determine if the equipment was capable of measuring the small change.

Repeatability--Drag measurements were made several times under varying ambiant conditions. Results obtained were compared to determine the repeatability of the system.

This investigation was carried out in the University of Minnesota's 3$\frac{3}{4}$ inch by 5$\frac{1}{4}$ inch subsonic wind tunnel.

EQUIPMENT

The direct force measuring apparatus evaluated was essentially a flat plate, the major portion of which consisted of a floating test panel. As drag forces were exerted on the plate by the airstream, the floating section applied a force against cantilevered springs. Strain gages mounted on these springs measured the deflection which was easily calibrated as a force. This device was mounted vertically along the centerline of the wind tunnel test section so that both sides of the plate were wetted by the airstream as shown in Fig. 1a. A general description of the construction of the equipment is given below. The reader is referred to Ref. 6 for details.

The apparatus consisted of an inner core to which two test panels were mounted and an outer core upon which frame plates were attached. The inner core was suspended in the outer core by two 0.037 inch piano wires as shown in Fig. 2. Roller bearings on the upper and lower edges of the inner core restricted its movement to the fore and aft direction. Frame plates of polished 0.25 inch aluminum sheet were attached to the outer core and completely surrounded the test panels. Both the inner and outer cores were constructed from 0.50 inch aluminum stock. Test panels of 0.25 inch thickness would then fit flush with the surrounding frame plates when mounted on the inner core. Adjustments on the

suspension wires and the frame plates permitted the air space between the frame and test panels to be set. This gap was 0.002 inches at the front with no displacement due to friction forces, 0.010 inches top and bottom, and 0.030 inches at the rear to allow for plate movement during drag measurements. The roller bearings on the inner core acted against set screws in the frame plates. This allowed the removal of any side-play of the inner core and test panels with respect to the frame. The apparatus with frame plates and test panels installed is shown in Fig. 3.

All points of contact between the inner and outer core were electrically insulated. An ohmmeter was placed in a circuit connecting the inner and outer cores. Any contact between the test panels and the frame plates would complete the circuit giving an indication on the ohmmeter. In this way any binding or rubbing in the system was immediately apparent.

Static pressures in the front and rear gaps were measured by taps in the outer core. The location of these taps can be seen in Fig. 2. In the original equipment the pressure leads from the leading edge were manifolded, as were the trailing edge taps, to give an average pressure. In this investigation all pressure taps were connected to individual tubes on the manometer bank.

A streamlined wooden nose-piece was attached to the leading edge of the outer core to provide a smooth flow of air onto the test panels. Two types of distributed

roughness were used to cause transition to turbulent flow--crepe masking tape, and 3M No. 150 emery paper. The first three inches of the wooden nose piece were covered for both types.

Two sets of test panels were used, one of 0.25 inch plate glass, and the other 0.25 inch polished Alclad sheet. The panels were 39.625 inches long and 29.500 inches wide. This gave a total wetted test area of 16.235 square feet. Crocus cloth, rotten stone, and jeweler's rouge were used to polish the aluminum plates. Although smooth to the touch, many scratches in the surface were visible. The glass panels were used with the original surface and also spray-painted with DuPont Duco Hi Speed Primer Surfacer No. 80 (red oxide). The roughness of the three surfaces was measured with a Brush Surface Analyzer. Sample records obtained are shown in Fig. 4. The stylus of the Brush Surface Analyzer moves back and forth over a distance of 3/16 inch. As the stylus reverses direction, a trace is made similar to a large roughness element. To avoid confusing these traces with surface roughness, the positions where the stylus reversed direction have been marked with arrows.

Waviness in the plates was roughly checked by means of a machinist's straightedge. None was found in the direction of flow. The test panels were mounted on the inner core with steel clips cemented on the inside surface. This allowed the test surface to remain unmarred by any attachment screws.

The rearward force produced by the airstream on the panels acted against two cantilevered steel spring bars (Figs. 2 & 5). These were arranged so that only the more flexible spring was engaged over the first 0.01 inches of displacement, at which point the second, stiffer spring was engaged. With this method greater sensitivity was attained in the lower force range. The original springs in the apparatus were designed to resist a load of 48 pounds for a 0.030 inch rearward movement of the plate. Early investigations showed the maximum forces encountered were on the order of five pounds. To achieve greater sensitivity on the strain indicating device, the weaker spring was redesigned to carry six pounds for a 0.030 inch deflection. The stiffer spring was designed to deflect 0.030 inches under ten pounds load but could be positioned to engage at any point from 0 to 0.030 inches of rearward plate travel. In this way the springs could be adjusted for maximum loads over a range of six pounds to 16 pounds. It was felt that this arrangement would give maximum outputs to the strain measuring device over the greatest range while not restricting the maximum permissible load. Appendix A contains the detailed redesign of the springs.

Baldwin A-7 strain gages mounted on the front and rear of the springs measured the strain which was read on a Baldwin SR-4, Model K, strain indicator. The gages were wired to provide temperature compensation as shown in Fig. 5. Due to the greater sensitivity of the redesigned springs,

the system showed considerable effect from tunnel vibration. These vibrations were analyzed with a Brush amplifier-recorder. Frequencies of from five to seven cycles per second were found to be predominant over the velocity range to be used. These oscillations were effectively filtered by placing an inductance and capacitance in the galvanometer circuit of the SR-4 strain indicator as shown in Fig. 5.

The total pressure probe used to survey the boundary layer is shown in Fig. 1b. The impact tube was made from 0.035 inch steel hypodermic needle flattened to obtain an inside diameter of 0.015 inches. The lower surface was filed to a thickness of 0.001 inches. Movement of the probe through the boundary layer was controlled by a Selsyn transmitter and receiver. An ohmmeter was placed in a circuit connecting the plate and the impact tube. As the tube was moved away from the surface, the circuit was broken. This method was used to establish the initial probe position on the surface.

The test apparatus was mounted in the University of Minnesota's 18 in. by 54 in. subsonic wind tunnel. This tunnel is a return flow type having a closed filleted rectangular test section bled to atmospheric pressure. Static pressure rings located upstream of the contraction cone and upstream of the test section were used to measure the dynamic pressure at the test section entrance. This pressure was read on a U-tube manometer and was used to maintain tunnel speed. This tunnel operated over a speed range of

zero to 200 miles per hour. The turbulence level in the tunnel was not determined but known to be high.

PROCEDURE

After the inner core with the test panels attached had been mounted in the outer core, the surface was carefully cleaned and polished with a dry cloth. Since the loads anticipated for the test panels used were not expected to exceed six pounds, the backup spring was moved away from the test panels so that it would not be engaged during the runs.

The first test was made on the polished aluminum plates with the leading edge of the wooden nose section covered with masking tape. Data were taken at four tunnel velocities--$U \cong 64$ ft/sec., $U \cong 143$ ft/sec., $U \cong 231$ ft/sec., and $U \cong 286$ ft/sec. Boundary layer surveys were made just forward of the leading edge gap at the center and two inches from the top and bottom of the test panel. A sufficient number of pressures were taken through the boundary layer to determine the character of the flow. This procedure was repeated at the trailing edge and for both test panels. The effect of the gap on the pressure profiles was investigated by comparing results obtained one-half inch ahead and one-half inch behind. No effect could be noted with the equipment used. This result was consistent with those obtained by Dhawan[5].

The test section static pressure and barometric pressure were recorded for each run. Wet and dry bulb temperatures were taken in the test section by inserting thermometers into the pressure equalizing slot at the downstream end of the test section. These temperatures were taken at the beginning and end of each run, the average being used for computational purposes.

All force measurements were made with the total pressure probe apparatus removed from the tunnel. The tunnel was brought to the highest test velocity and the pressures at the leading and trailing edges of the plate recorded. The reading on the strain indicator was taken along with the wet and dry bulb temperatures. The velocity was then reduced to the next lower test speed and the procedure repeated. In this way the overall change in air temperature during the run was held below four degrees Fahrenheit which minimized any temperature effect on the strain gage readings. After the data at the four velocities were obtained, the tunnel was immediately stopped and the balance system calibrated. This was accomplished by attaching twine to the surfaces of the test panels. The twine led over a low-friction pulley mounted at the rear of the outer core. Weights were then hung on the twine and the calibration curve drawn. A typical curve is shown in Fig. 6. During the test run and the balance calibration, the ohmmeter in the warning circuit was observed to detect any rubbing in the system. Upon completion of the balance

calibration, the test panels were again cleaned and the drag measurements repeated.

In the same manner as on the aluminum panels, boundary layer surveys were done at the leading and trailing edges on the glass test panels. In addition, the boundary layer thickness was determined at the center and two inches from the top and bottom of the test panels at stations located one-third and two-thirds down the length of the panels. The total pressure probe was moved outward from the plate until no change in pressure was noted by further travel into the free stream. This point was taken as the boundary layer thickness. A slightly different procedure was required in finding the point at which the probe left the surface of the plate. Since the electrical method described earlier in this report could not be used, it was necessary to place the probe firmly on the surface at the start of each run. With the tunnel running at the test velocity the probe was moved away from the surface, and it was noted at what point the pressure began to increase. This was then taken as the surface position. The force measurement procedure was identical to that performed on the aluminum plates. The warning circuit was maintained by coating the edges of the glass panels with conducting paint. This series of runs used emery paper on the nose section to obtain turbulent flow.

Two more conditions were investigated. The forces on the glass plate with the emery paper covered with masking tape were measured, and the forces on the painted glass plates with emery paper on the nose section were found.

All pressures were read with reference to the test section static pressure. A tube on the manometer bank was left open to atmospheric pressure and was also read with reference to the test section static pressure. This permitted any pressures to be converted to an atmospheric reference when necessary.

RESULTS AND DISCUSSION

A preliminary investigation was made to determine if the data measured on the drag balance were consistent for each set of panels tested. It can be seen from the approximate turbulent skin-friction equation,

$$C_F = \frac{D}{\frac{\rho}{2}U^2L} = \frac{0.072}{\left(\frac{\rho UL}{\mu}\right)^{1/5}}$$

that the drag on a flat plate varies as the velocity to the 9/5 power (Ref. 8). Fig. 7 shows the measured drags, corrected for the end pressures on the floating section, plotted versus $U^{9/5}$. The near linear relation between drag and $U^{9/5}$ indicates that no large errors had been incurred due to malfunctioning of the drag balance system during any particular run.

Fig. 7 shows data for only three velocities for the aluminum plates. The pressure profiles showed portions of the plate in laminar flow at a velocity of $U = 64$ ft/sec. This test used the masking tape on the nose piece. Subsequent tests on the other surfaces used the rougher emery paper which produced turbulent flow at all four test speeds. Distributed roughness was chosen to produce transition to turbulent flow since the effect on the flow disappears more rapidly for a trip of this type (Ref. 9).

The drags were reduced to coefficient form as outlined in Appendix B. For purposes of comparing the results from the direct force measurements and those obtained by Readdy[7] from the boundary layer survey, the coefficients and Reynolds number were based on the length of the test panel as the characteristic length (L = 3.30 ft.). Fig. 8a shows the results obtained on the glass test panels with the emery paper on the nose piece. The agreement is fair. The maximum difference between the two curves over the velocity range tested is five per cent. This difference could easily be the result of the experimental scatter for the two methods of drag measurement.

The coefficients obtained for the Alclad test panels are presented in Fig. 8b. A comparison of the skin friction coefficients for the Alclad panels with those obtained on the glass panels (Fig. 8a) show a considerable drag reduction on the Alclad. The traces of surface roughness in Fig. 4 indicate that the Alclad panels are rougher and should produce higher drag coefficients than the glass panels. The aluminum panels were tested with masking tape on the nose piece while the glass used emery paper. It was felt that the primary effect of changing the nose roughness would be to alter the Reynolds number (based on a characteristic length from the virtual origin* of an equivalent flat plate).

*The virtual origin is the location of the leading edge of an equivalent smooth flat plate with all turbulent flow that would produce the same flow conditions at the leading edge of the test panels as those of the roughened nose piece (Ref. 9).

This in turn would compensate for any change in measured drag and the coefficients obtained with both types of nose roughness would lie on the same curve. To verify this assumption drag measurements were made on the glass plate with the emery paper covered by masking tape. When the coefficients for the glass plate with the two types of nose roughness were corrected for the effect of the nose piece, as described in Appendix B, the agreement was found to be within two per cent. From this it was concluded that the low drags measured on the Alclad test panels did not result from changing the nose roughness.

The results obtained from the boundary layer survey also indicate this. The coefficients found for the Alclad panels are on the same order of magnitude as those measured for the glass panels, Fig. 8a and b. Some other direct force measurement results were available for the Alclad panels (obtained by Hendley[6]). This work used a 0.0625 in. diameter trip wire just ahead of the leading edges of the test panels to obtain turbulent flow. While the character of the flow was not duplicated in the two tests, some correlation in the results can be expected. It can be seen in Fig. 8b that these results roughly compare to those obtained from the boundary layer survey. From this it appeared that the results measured by this author are incorrect for the Alclad test panels.

The first tests conducted used the Alclad panels. As more experience was gained with the apparatus, it was found that the side play set screws should be tightened only enough to remove any lateral motion of the plates and not to force alignment with the surrounding frame plates. This was done for the glass panels and alignment with the frame plates attained by placing shims under the frame plates. It is believed that the improper mounting of the inner core produced the incorrect results obtained for the Alclad test panels.

The comparison of the coefficients for the painted panels is shown in Fig. 9a. The agreement is within 8.5 per cent. The coefficients determined by the momentum loss were computed from a limited boundary layer survey (Ref. 7). The surface roughness varied considerable over the panel, and it is believed that better correlation would have been attained had a complete survey been done.

Fig. 9b presents a comparison of the coefficients determined from the direct force measuring apparatus for the glass and painted panels. Higher coefficients were found for the painted surface at all velocities which indicated that the equipment is capable of measuring small increases in surface roughness.

In order to compare the results obtained from the force measuring device with existing theory, it was

first necessary to determine if the flow conditions on the apparatus approximated the assumptions made in the theoretical analysis, i.e. a smooth flat plate at zero incidence with no pressure gradient, and, for the case investigated, turbulent flow from the leading edge.

The glass plate was believed to best simulate the smooth plate. The roughness trace in Fig. 4 shows an average roughness element height of approximately three micro-inches and was consistent for varying locations over the sample tested. The glass plate was then considered to be a hydraulically smooth plate.

The plates were checked for curvature or waviness in the direction of flow with a machinist's straightedge. None was noted and the plates were assumed to satisfy the condition of being flat.

Since the balance apparatus was mounted along the centerline of the test section, it was assumed that the angle of attack was near zero.

An indication of the pressure variation along the plate was obtained from the variation in the free stream dynamic pressure measured during the boundary layer surveys. Fig. 10 shows this variation along the center

of the plate. Except for the low speed test, U = 64 ft/sec., the maximum pressure variation was less than three per cent. The large variation for the low velocity resulted from the large percentage reading error of the manometer and not from an excessive pressure variation. It was felt that this pressure variation would not be large enough to effect the values of the skin friction coefficients.

The average boundary layer growth along the plate was computed and compared to the theoretical growth given by the expression,* (Blasius)

$$\delta = \frac{0.37x}{(R_{N_x})^{1/5}}$$

These results are presented in Fig. 11. The boundary layer growth does approximate theory for the two lower test velocities, but the roughness on the nose piece has considerable effect at the higher speeds. Hence, it appears that the boundary layer growth only roughly approximates that of the theoretical boundary layer.

To determine if the flow on the plate was fully turbulent, the dynamic pressure profiles at the leading and trailing edges of the test panels were plotted as dimensionless velocity profiles and compared to the $\frac{1}{7}$ power distribution law, Figs. 12-15. The agreement is excellent for U = 64 ft/sec., but becomes poorer as

*The length x is measured from the virtual origin of the plate. The method used to locate the virtual origin is described later in this report.

the speed is increased. Better agreement was obtained at the trailing edge than at the leading edge. It was concluded from this that the higher velocities did not give sufficient time for the effect of the roughened nose piece to disappear. Generally, the agreement is good for the entire speed range, and although the higher velocities are not fully developed, are close enough to satisfy the requirement of turbulent flow.

The results obtained above indicate that the flow on the test panels approximately satisfies the conditions imposed in the theoretical analysis. If the coefficients obtained from the test apparatus are corrected to an equivalent flat plate with turbulent flow starting at the leading edge, agreement with calculated coefficients should be expected if the balance measures the drag correctly.

In order to correct the results to fully turbulent theory, the virtual origin of the equivalent flat plate must be determined. This is difficult due to the unknown effects of the emery paper and the favorable pressure gradient along the streamlined nose piece. An approximate distance from the leading edge of the test panel to the virtual origin was obtained by calculating the length of flat plate with turbulent flow from the leading edge that would be required to produce a boundary layer thickness equal to the value measured at the

leading edge of the test panel. The following expression was used,

$$\delta = \frac{0.37x}{\left(\frac{\rho U x}{\mu}\right)^{1/5}}$$

The length from the virtual origin to the trailing edge of the test panel was then used as the characteristic length. These characteristic lengths are functions of velocity and were calculated for each of the four test speeds. The values obtained agreed within two per cent with values calculated by Readdy[7] using the momentum loss at the leading edge. The additional drag that would be produced by that portion of the plate from the virtual origin to the leading edge of the plate was computed from the empirical relation (Ref. 2),

$$C_F = 0.455(\log_{10} R_N)^{-2.58}$$

In this way both the Reynolds number and the skin friction coefficient were corrected to an equivalent flat plate with turbulent flow from the leading edge. Details of these corrections are given in Appendix B.

The corrected skin friction coefficients are shown in Fig. 16. The agreement with the empirical skin friction formula given above is good. The maximum deviation from theory was only 4.5 per cent. From this it was concluded that the apparatus does measure the skin friction drag of a flat plate at zero incidence.

All direct force measurements were repeated over a period of time to determine if the equipment would produce consistent results. The maximum percentage deviation of the measured drag was two per cent.

CONCLUSIONS AND RECOMMENDATIONS

The direct force measuring device was investigated to determine (1) its ability to measure skin friction drag, (2) if the flow conditions on the test panels satisfied the conditions imposed for existing flat plate theory, (3) the ability of the equipment to measure small increases in surface roughness, and (4) the repeatability of the equipment.

(1) Results show that the apparatus will measure the skin friction forces on the test panels if extreme care is exercised in mounting and aligning the floating section in the outer frame. Large errors can be incurred if the floating section is restrained in any way by the contact at the roller guide bearings.

(2) The flow over the test panels approximates the conditions of fully turbulent flow over a flat plate at zero incidence with zero pressure gradient. The coefficients determined from the apparatus can be corrected to fully turbulent flat plate theory.

(3) Small increases in surface roughness can be detected with this apparatus.

(4) The equipment shows excellent repeatability when no adjustments to the plate alignment and

mounting are made. This would indicate that the apparatus is well suited to "sorting" surfaces of varying roughness if the surfaces can be applied to the same test panels, i.e. paint.

The question will arise for any further tests with this device as to whether the floating section has been mounted correctly. It is recommended that the results be reduced to a coefficient form comparable to the glass plates in this investigation. A comparison with these results will indicate any large errors due to improper mounting of the equipment.

It is further recommended that the number of static pressure taps that measure the gap pressure at the leading and trailing edges of the test panels be increased. The force correction for the end pressure was as high as 20 per cent of the measured drag for some runs. Hence, it seems desirable to have more accurate information on the pressure variation in the gap.

APPENDIX A

Design of the Strain Gage Springs

The strain gage springs were designed as cantilever beams and were constructed of steel (Fig. 5). Their design was greatly restricted by the various conditions that were to be satistied. It was felt desirable that, using as SR-4 strain indicator, the system should be capable of measuring a one pound force with 1.5 per cent accuracy. It was estimated that the strain indicator could be read accurately to the nearest two micro-inches per inch. Hence, to obtain the accuracy desired, a one pound load must produce a stress of 3,800 lbs/in^2 at the strain gage.

In view of preliminary experiments carried out with this apparatus, it appeared doubtful that the maximum force measured would ever exceed sixteen pounds with most loads occuring below six pounds. The maximum acceptable displacement of the test panels from the static position was 0.030 inches. It was desired to design one spring to carry six pounds and the other to carry ten pounds when deflected 0.030 inches. From this the spring constants were determined--primary spring, $k = 200$ lbs/in and the back-up spring, $k = 333$ lbs/in. The point of engagement of the back-up spring was adjustable so that the loads producing the maximum permissible

deflection could be varied from 6 to 16 pounds. In this way the maximum sensitivity was maintained over the greatest possible test range.

Since it was necessary to mount these springs in the same location as the original springs, the length of the cantilevered portion was fixed at four inches. A further restriction was the minimum length of the "necked-down" portion of the springs. This minimum length was 0.50 inches to accommodate the A-7 strain gages.

Four quantities remained that could be varied--the width of the bar, the two thicknesses, and the length from the free end to the position of the strain gages. By trial a suitable combination was obtained to meet the requirements stated above.

Primary Spring:

E = 28.5×10^6

σ_{max} = 50,000 lb/in^2

b = width--taken as 0.375 in.

L_1 = length from free end to center of strain gage location--taken as 2.50 in.

σ = desired stress at strain gage = 3,800 lb/in^2

δ' = spring deflection = 0.030 in.

t = thickness of spring = in.

subscript 1--refers to "necked down" portion of spring

subscript 2--refers to the remaining portion of spring

The stress at the strain gage was,

$$\sigma = \frac{My}{I} = \frac{PL_1 \frac{t_1}{2}}{\frac{bt_1^3}{12}} = \frac{6PL_1}{bt_1^2}$$

$$3800 = \frac{(6)(1)(2.5)}{(.375)t_1^2}$$

$$t_1 = 0.102 \text{ in.}$$

$$\therefore I_1 = \frac{bt_1^3}{12} = \frac{(.375)(.102)^3}{12} = 0.0000336 \text{ in}^4$$

The deflection of the beams could be expresses as:

$$\delta' = \int_0^L \frac{PL^2 dL}{EI} = \left[\frac{L^3}{3EI_2}\right]_0^{2.25} + \left[\frac{L^3}{3EI_1}\right]_{2.25}^{2.75} + \left[\frac{L^3}{3EI_1}\right]_{2.75}^{4.00}$$

Everything in this equation was known except I_2.

$$I_2 = 0.00369 \text{ in}^4$$

$$t_2^3 = \frac{12I_2}{b} = \frac{(12)(.00369)}{(.375)} = 0.0118 \text{ in}^3$$

$$t_2 = 0.226 \text{ in.}$$

The back-up spring was designed in a similar manner as the primary spring. The resulting dimensions were: $b = 0.300$ in, $L = 2.50$ in, $t_1 = 0.115$ in, and $t_2 = 0.648$ in. A comparison of the calibration curves for the original and re-designed springs showed that the sensitivity of the force measuring equipment had been increased by a factor of ten.

APPENDIX B

Sample Data Reduction

Sample calculations are shown for the glass test panels with emery paper on the nose piece for U=143 ft/sec. The date obtained during the test is presented below.

q_m	r	P_B	t_D	t_w	ΔP
5.0	1605	29.21	92	63	0.25

where:

q_m = dynamic pressure set on the tunnel control manometer--in. of alcohol

r = reading on the strain indicator

P_B = barometric pressure--in. of Hg

t_D = dry bulb temperature--^oF.

t_w = wet bulb temperature--^oF.

ΔP = difference between test section and atmospheric pressure--in. of alcohol

These data were augmented by the static pressures at the leading and trailing edges of the test panel, the pressure profiles through the boundary layer, and the calibration curve of strain indicator readings versus load in pounds.

Calculation of Skin Friction Coefficient:

The drag on the panels was found from the calibration curve--D = 1.43 lbs. The static pressures on the leading edge of the test panel were averaged, as were the pressures on the trailing edge, and the pressure difference between the two found--$\Delta P'$ = 0.20 in. of alcohol = 0.84 lbs/ft^2. The area of the end of the floating element was A = 0.205 ft^2. The drag could then be corrected for the end pressure.

$$D' = D - A\Delta P'$$

$$D' = 1.43 - (0.205)(0.84) = 1.26 \text{ lbs.}$$

The force from the end pressure was found to act downstream in all runs. Thus, the drag correction was always negative.

The free stream dynamic pressure in the test section, q, was obtained by averaging all the values obtained during the boundary layer survey, q = 5.27 in. of alcohol = 22.15 lbs/ft^2. This value differed from the tunnel manometer reading (q_m = 5.0). Therefore, q_m was used only to set the tunnel speed and not for computations.

For the comparison of the results obtained by direct force measurement with those from momentum loss, the length of the test panel was used as the characteristic length. Then the skin friction coefficient could be written,

$$C_F = \frac{D'}{qS}$$

$$C_F = \frac{1.26}{(22.15)(16.23)} = 0.00351$$

where S is the total test panel area.

Calculation of Reynolds number:

The density in the test section was computed by correcting the atmospheric pressure for the difference between test section and outside pressure--

$\Delta P = -0.25$ in. of alcohol $= -0.01$ in. of Hg.

$$P'_B = P_B + \Delta P$$

$$P'_B = 29.21 - 0.01 = 29.20 \text{ in. of Hg.}$$

The tables of Ref. 10 were then used to obtain the density from the corrected barometric pressure, the dry bulb temperature, and the difference between the wet and dry bulb temperatures--$\rho = 0.00216$ slugs/ft^3. From ρ and q the free stream velocity, U, could be calculated.

$$q = \frac{\rho}{2} U^2$$

$$U = \sqrt{\frac{2q}{\rho}} = 143 \text{ ft/sec.}$$

Viscosity was found from the equation,

$$\mu = 2.270 \frac{T^{3/2}}{T + 198.6} \times 10^{-8}$$

$$\mu = 39.9 \times 10^{-8} \frac{\text{lb-sec}}{\text{ft}^2}$$

where T is the dry bulb temperature in degrees Rankine. Using the length of the test panel, $L = 3.3$ ft., for the characteristic length, the Reynolds number was computed.

$$R_N = \frac{\rho UL}{\mu}$$

$$R_N = \frac{(0.00216)(143)(3.3)}{39.9 \times 10^{-8}}$$

$$R_N = 2,560,000$$

Correction to Fully Turbulent Flat Plate Theory

In the computations presented above, the effect of the nose piece on the coefficient and the Reynolds number was not considered. In order to compare with flat plate theory, the following procedure was used.

The average boundary layer thickness at the leading edges of the test panels was found from the pressure profiles-- $\delta = 0.01817$ ft. The length of flat plate with turbulent flow from the leading edge that would be required to produce a boundary layer of this thickness was given by the equation,

$$\delta = \frac{0.37\ x}{\left(\frac{\rho U x}{\mu}\right)^{1/5}}$$

All quantities in this equation were known with the exception of x. Thus, the equation could be solved for this length--x = 0.683 ft. This established the virtual origin of the plate, and the new characteristic length was measured from this origin to the trailing edge of the test panels--L' = 3.99 ft. Then, the corrected Reynolds number became,

$$R_N = \frac{(0.00216)(143)(3.99)}{39.9 \times 10^{-8}} = 3,090,000$$

Since flat plate theory predicts the total drag on a plate from the leading edge, the drag measured

on the force measuring apparatus must be increased to include the drag from the virtual origin to the leading edge of the test panels. To accomplish this the Reynolds number based on the length x = 0.683 ft. was computed (R_{N_x} = 529,000) and used in the following equation to find a skin friction coefficient.

$$C'_F = 0.455 \, (\log_{10} R_{N_x})^{-2.58}$$

$$C'_F = 0.00505$$

The drag contributed by this portion was then found.

$$D'' = C'_F q S'$$

$$D'' = (0.00505)(22.15)(1.68) = 0.190 \text{ lbs.}$$

S' was the area of the portion of the plate from the virtual origin to the leading edge of the test panels--$S' = 1.68$ ft^2. These values of drag and area were for one side of the plate. To correct the skin friction coefficient to flat plate theory, twice this drag must be added to the measured drag and twice the area added to the test panel area since the measured values were for both sides of the plate.

$$C_F = \frac{D' + 2D''}{q(S + 2S')}$$

$$C_F = \frac{1.25 + .38}{22.15(16.23 + 3.36)} = 0.00376$$

REFERENCES

1. Goldstein, S., Low Drag and Suction Airfoils, Jour. Aero. Sci., April 1948.

2. Schlichting, H., Boundary Layer Theory, McGraw-Hill Book Company, Inc., New York, 1955.

3. Nikuradse, J., Laws of Flow in Rough Pipes, NACA TM 1292, November 1950.

4. Prandtl, L., Schlichting, H., Das Widerstandsgesetz rauher Platten Werft, Reederei, Hafen, (1934) pp. 1-4.

5. Dhawan, Satish, Direct Measurements of Skin Friction, NACA TN 2567, January 1952.

6. Hendley, A. C., Study of Optimum Gains in Skin Friction Coefficient in Turbulent and Laminar Flow for Different Qualities of Aircraft Finishes and the Design and Construction of Test Apparatus, M. S. Thesis, University of Minnesota, August 1955.

7. Readdy, F. J., The Determination of the Skin-Friction Drag of a Large Flat Plate of Different Finishes from Boundary Layer Investigation, M. S. Thesis, University of Minnesota, June 1956.

8. von Karman, T., On Laminar and Turbulent Friction, NACA TM 1092, September 1946.

9. Klebanoff, P. S., Diehl, Z. W., Some Features of Artificially Thickened Fully Developed Turbulent Boundary Layers with Zero Pressure Gradient, NACA TN 2475, October 1951.

10. Boehnlein, C. T., Air Density Tables, Engineering Experiment Station Technical Paper 17, University of Minnesota, Institute of Technology.

a - drag balance and boundary layer probe (glass panels)

b - boundary layer probe (painted panels)

Fig. 1 Test Apparatus and Boundary Layer Probe

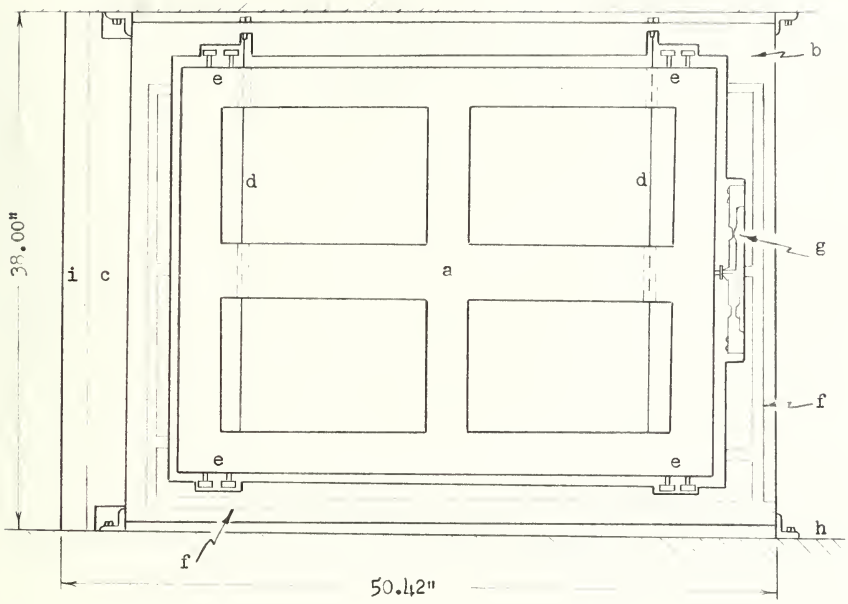

a - inner core

b - outer core

c - wooden nose piece

d - suspension wires

e - insulated roller bearings

f - channels for static pressure tap leads

g - strain gage springs

h - attachment angles

i - #150 emery paper

flow direction from left to right

Fig. 2 Test Apparatus With Test Panels and Frame Plates Removed

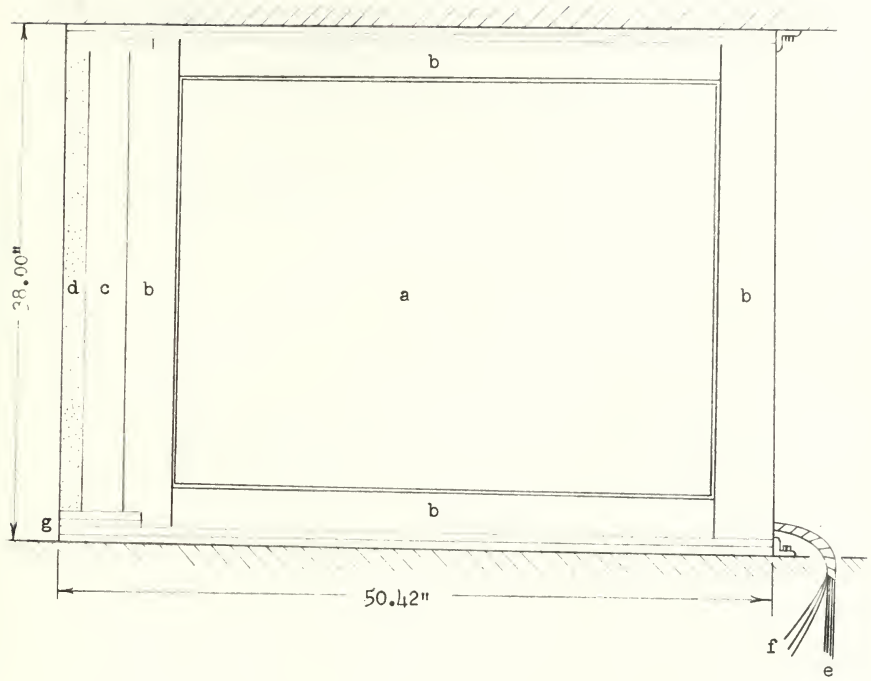

a - test panel - 39.62 x 29.5 in.

b - frame plates

c - wooden nose piece

d - #150 emery paper

e - pressure leads

f - strain gage leads

g - masking tape

flow direction from left to right

Fig. 3 Test Apparatus With Test Panels and Frame Plate Installed

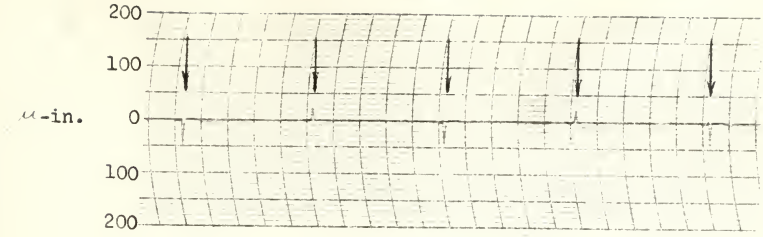

a - glass

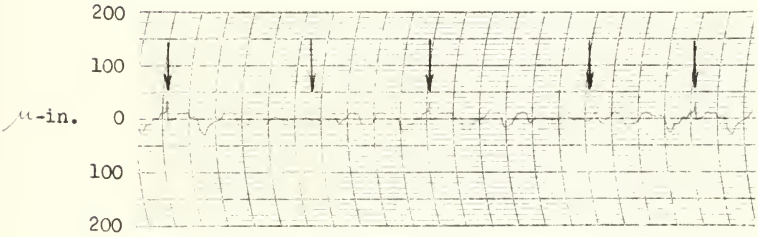

b - painted glass

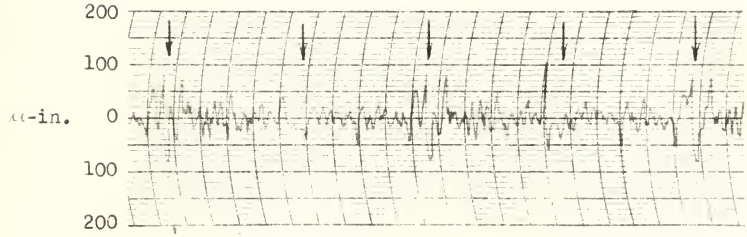

c - polished Alclad

Fig. 4 Sample Surface Roughness of the Test Panels

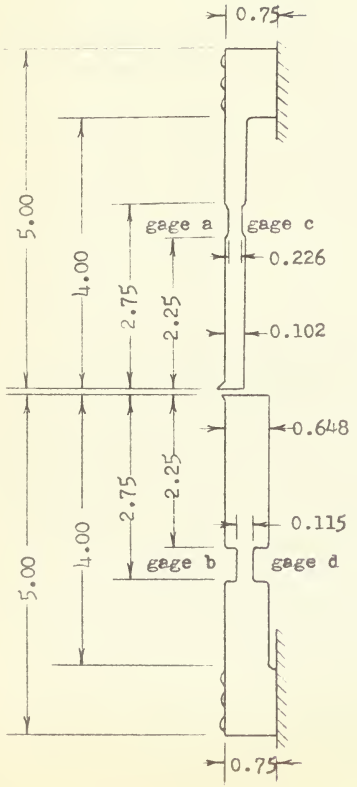

C - 24 μ-farads

L - 20 henries

G - galvanometer

R_1 - coarse bridge adjustment

R_2 - fine bridge adjustment

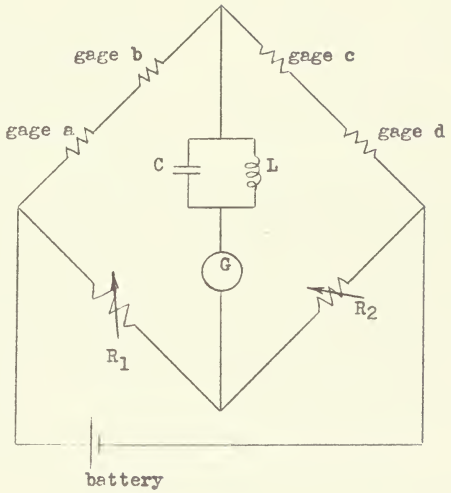

Fig. 5 Strain Gage Springs and Bridge Circuit

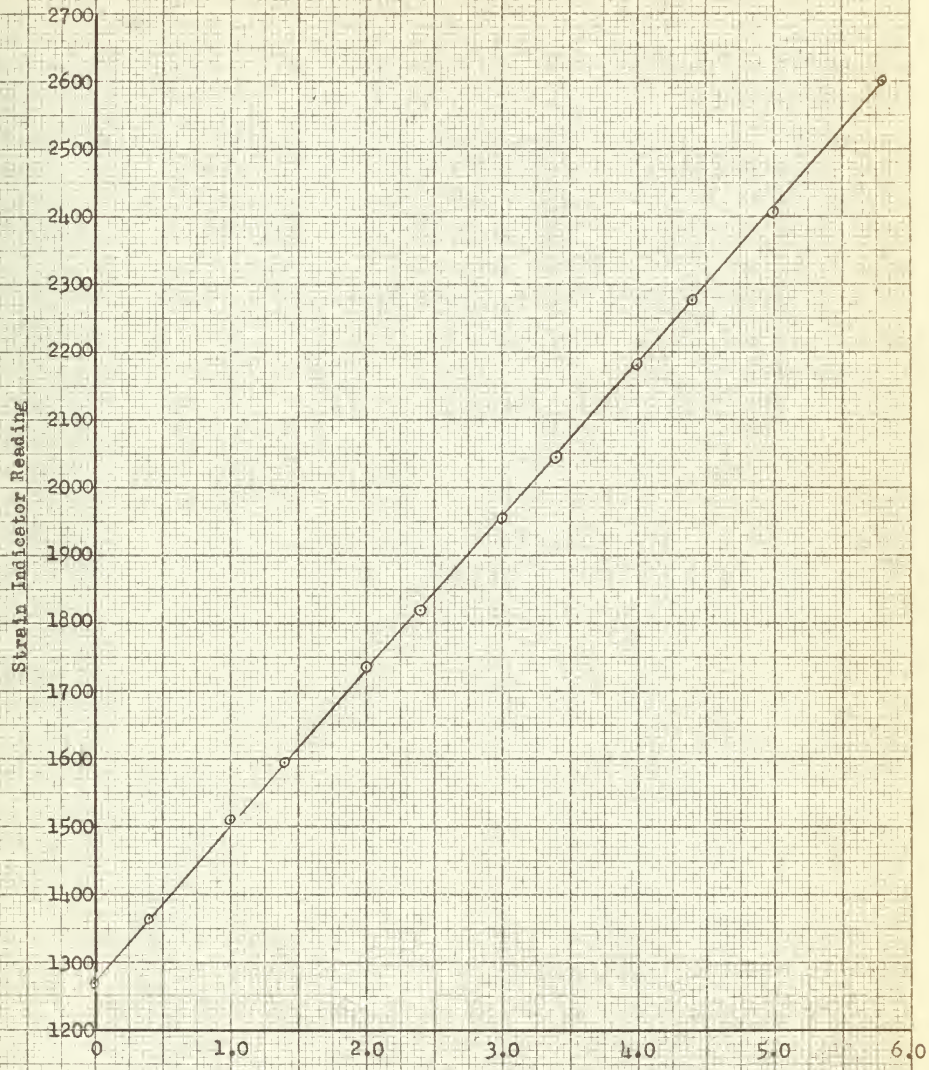

Fig. 6 Typical Strain Gage Calibration Curve

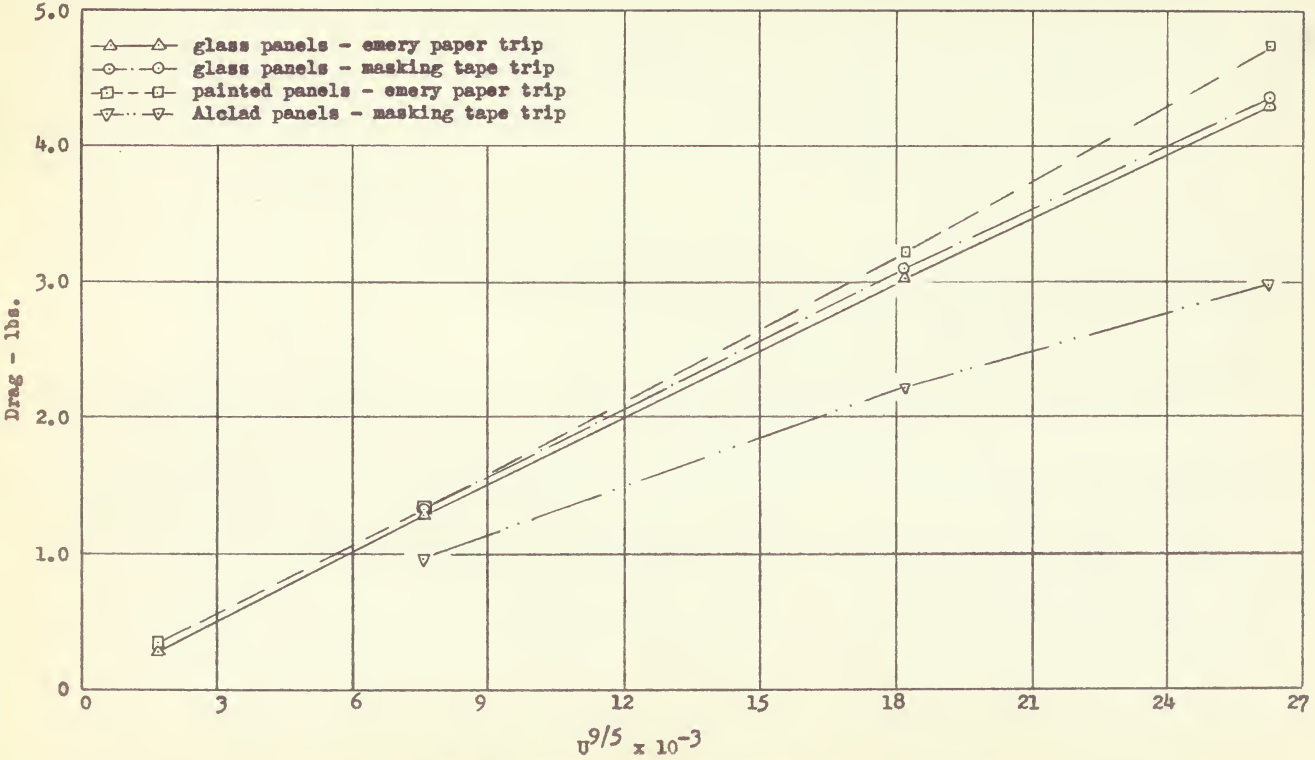

Fig. 7 Measured Drag Corrected for End Pressure

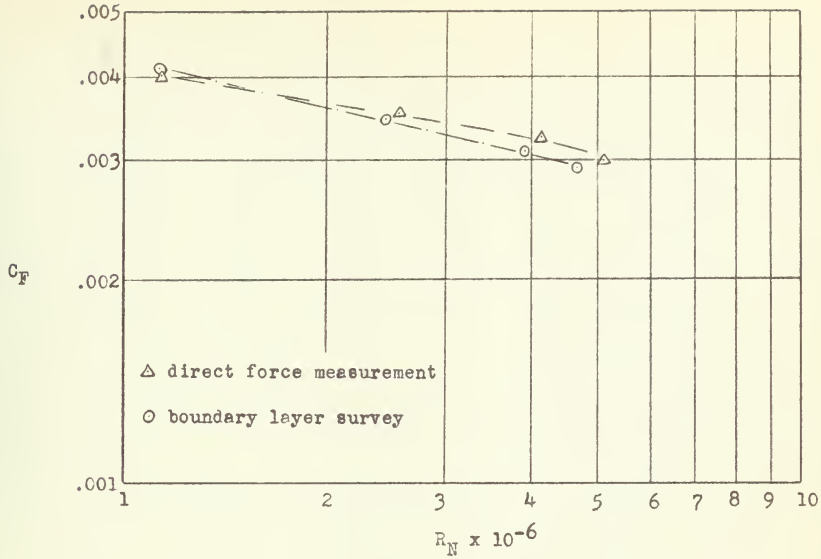

a - glass panels

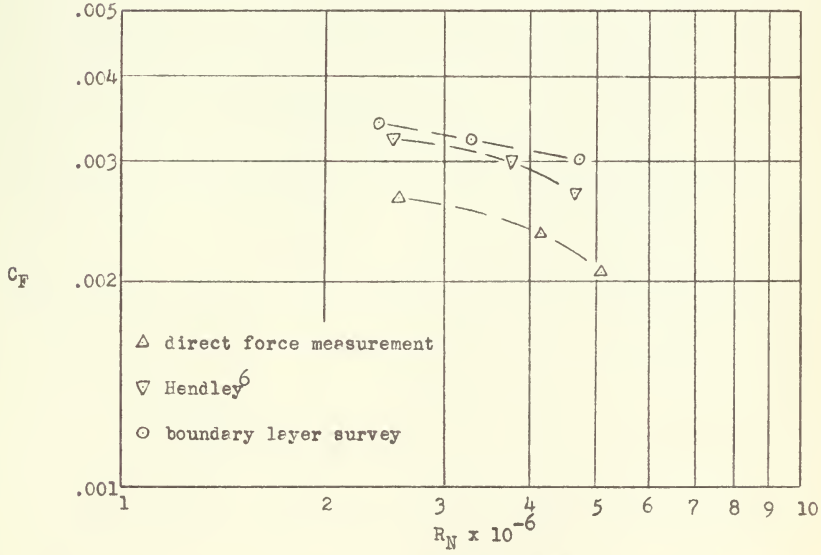

b - Alcled panels

Fig. 8 Comparison of Direct Force and Momentum Loss Measurements

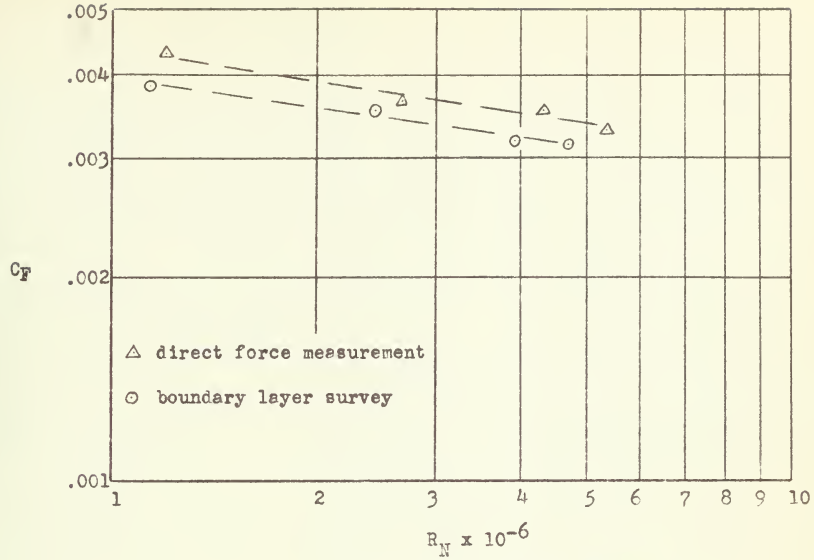

a - painted panels (glass)

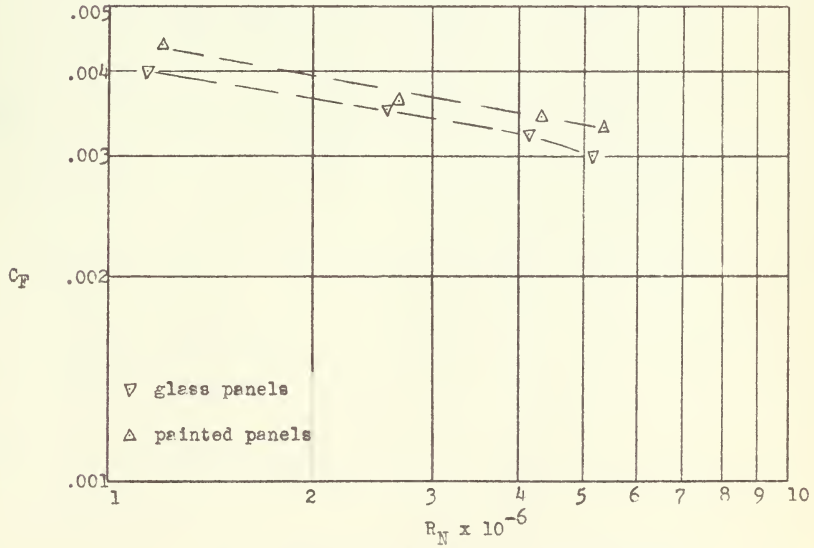

b - comparison of glass to painted panels

Fig. 9 Comparison of Painted Panels to Glass Panels and Momentum Loss Measurements

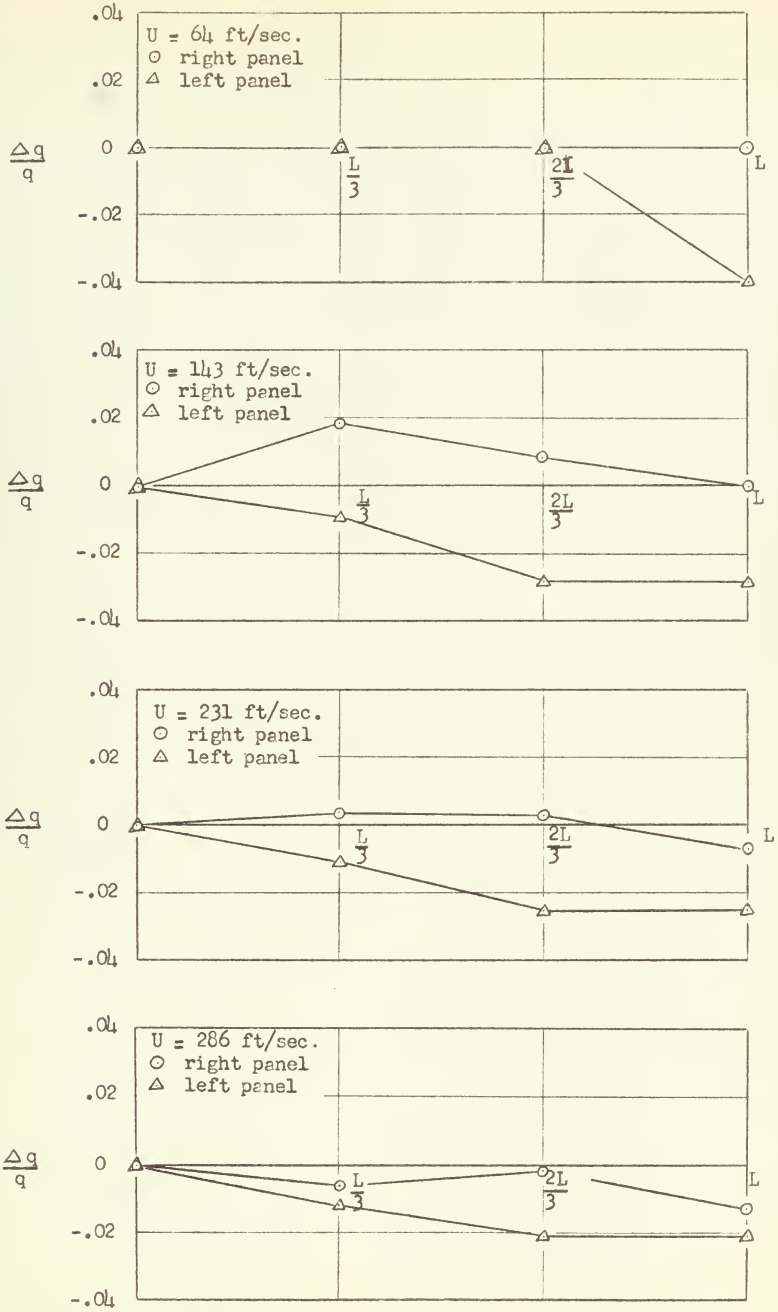

Fig. 10 Free Stream Dynamic Pressure Distribution Along The Center Of Test Panels (Test panel length L = 3.3 ft.)

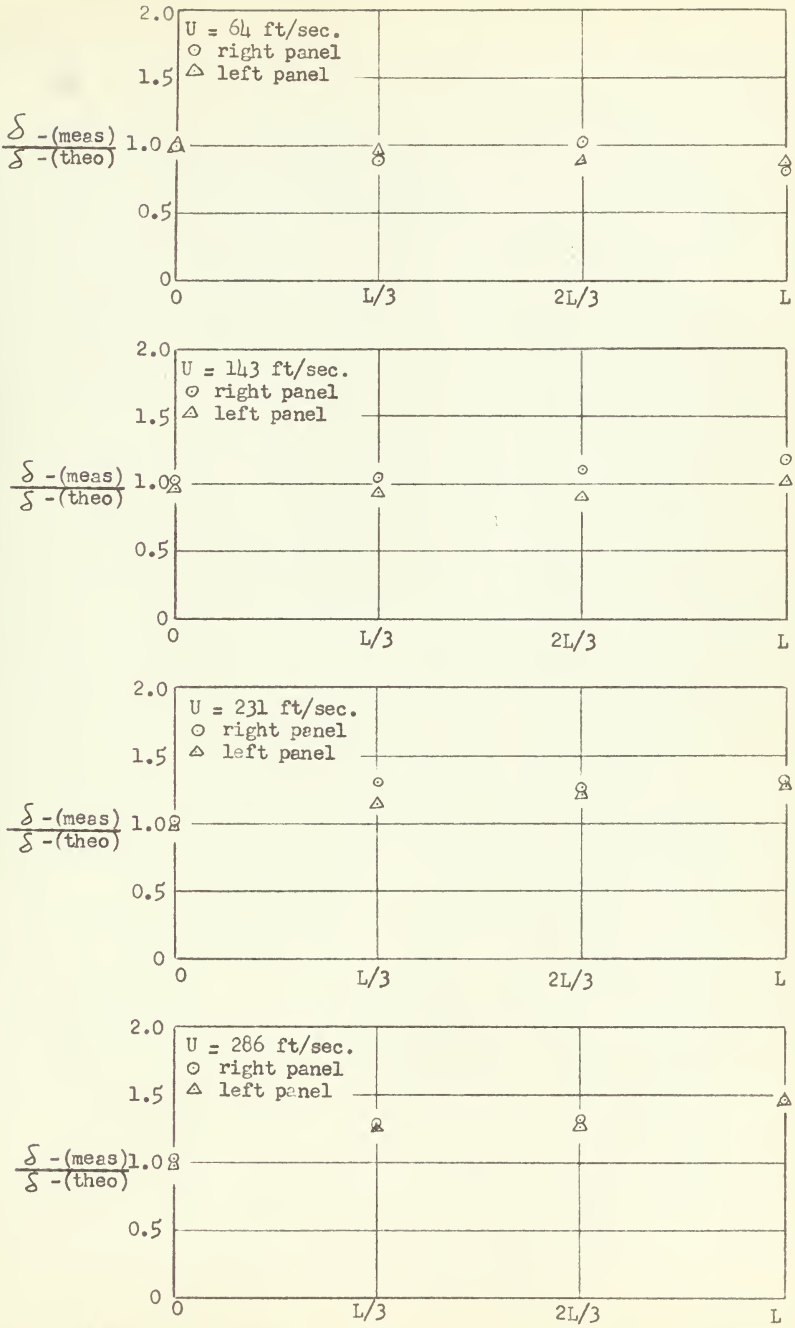

Fig. 11 Comparison of Theoretical and Measured Boundary Layer Thickness (Test Panel Length L - 3.3 ft.)

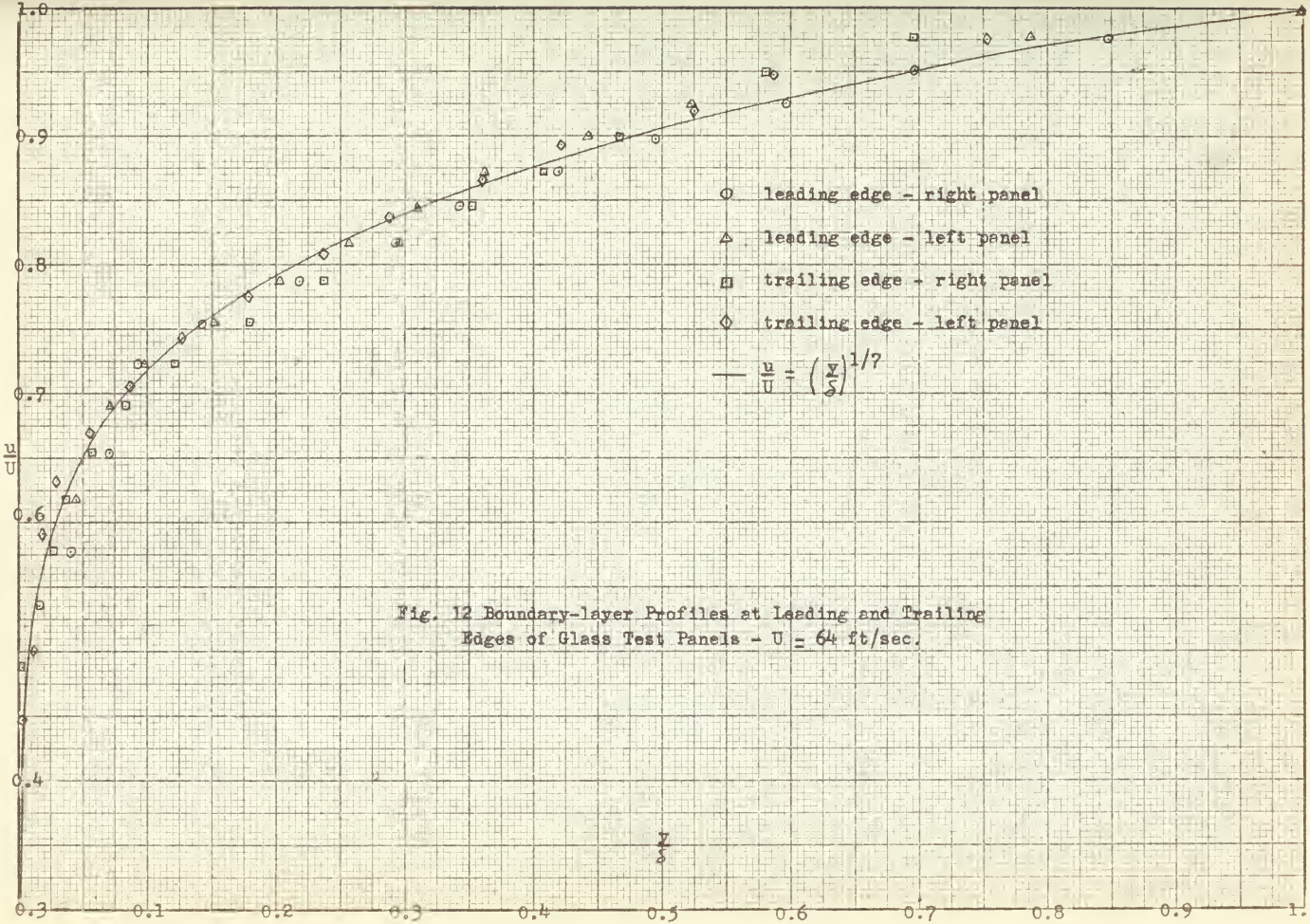

Fig. 12 Boundary-layer Profiles at Leading and Trailing Edges of Glass Test Panels - U = 64 ft/sec.

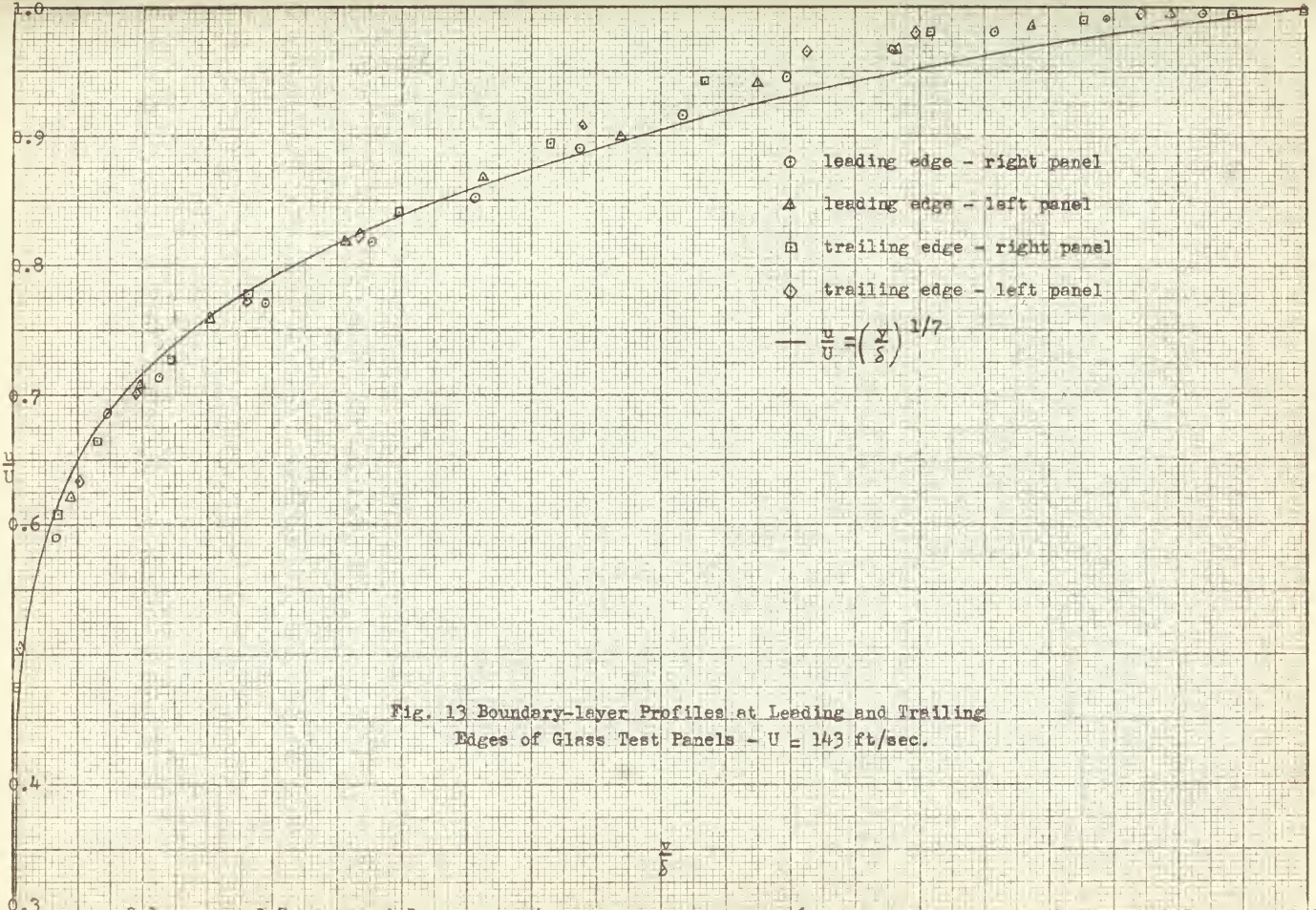

Fig. 13 Boundary-layer Profiles at Leading and Trailing Edges of Glass Test Panels - U = 143 ft/sec.

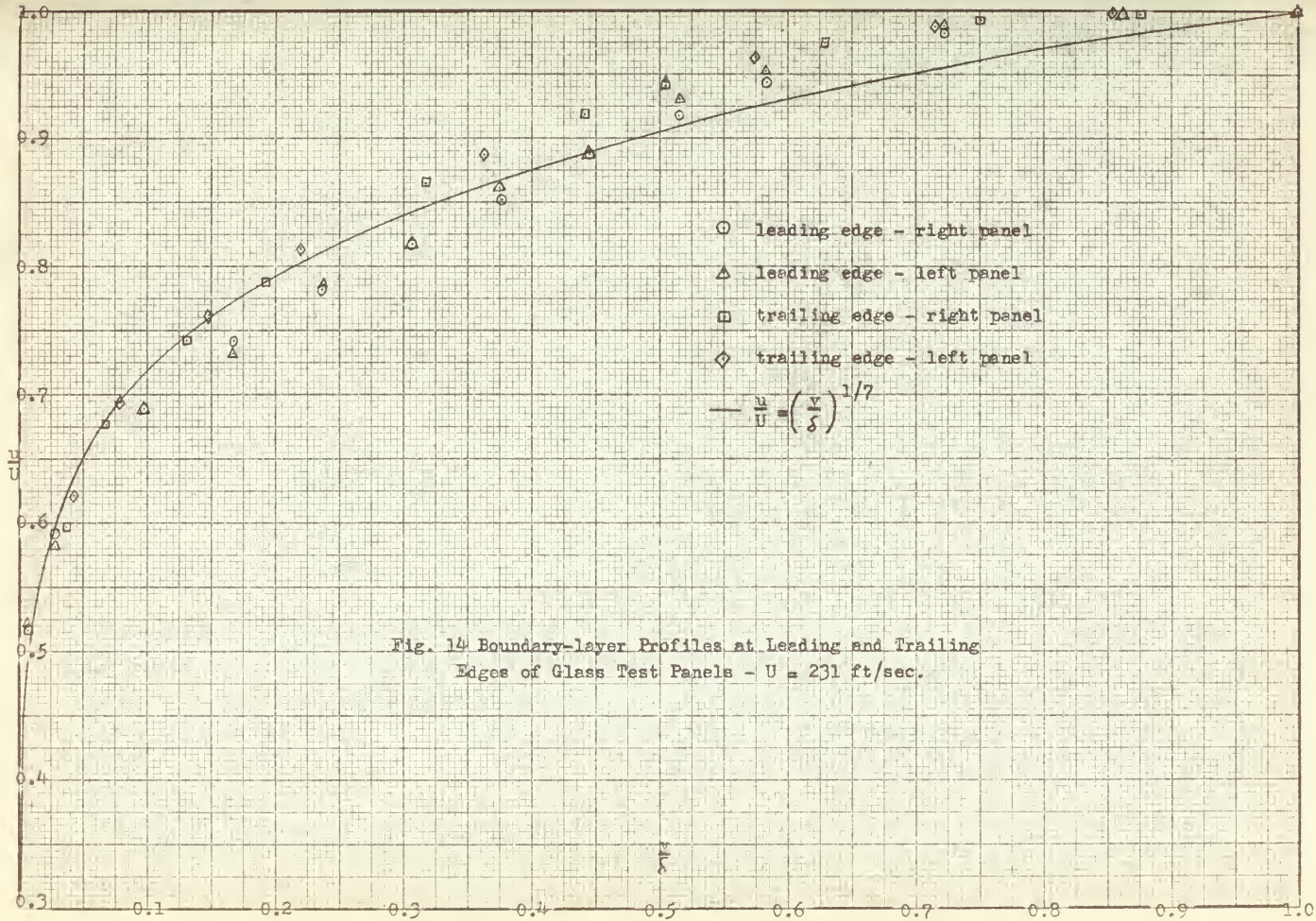

Fig. 14 Boundary-layer Profiles at Leading and Trailing Edges of Glass Test Panels - U = 231 ft/sec.

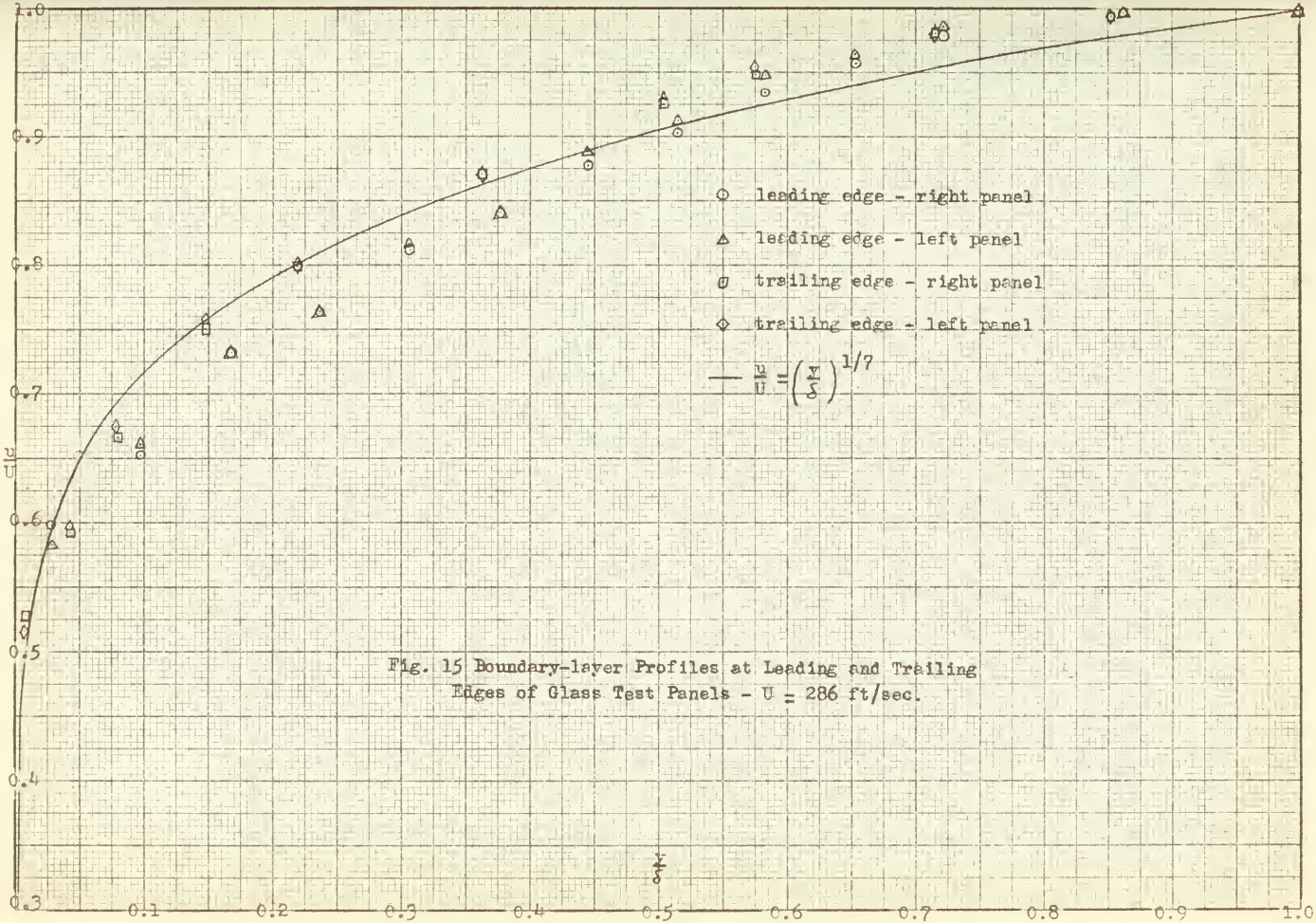

Fig. 15 Boundary-layer Profiles at Leading and Trailing Edges of Glass Test Panels - U = 286 ft/sec.

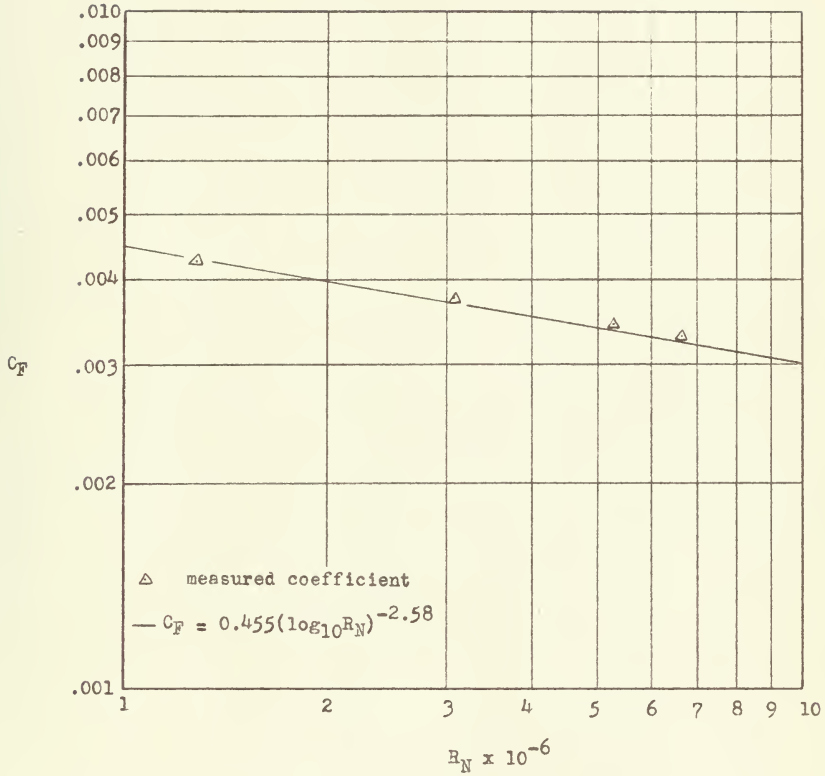

Fig. 16 Skin Friction Coefficient for the Glass Test Panels Corrected to Theory

Thesis 33154
W694 Wolff
An evaluation of equipment to measure directly the skin friction forces on a flat plate.